

Cooperative Folding of a Protein Mini Domain: The Peripheral Subunit-Binding Domain of the Pyruvate Dehydrogenase Multienzyme Complex

Shari Spector¹, Brian Kuhlman², Robert Fairman³, Elsa Wong²
Judith A. Boice³ and Daniel P. Raleigh^{2,4*}

¹Department of Physiology and Biophysics, State University of New York at Stony Brook
Stony Brook, NY 11794-8661
USA

²Department of Chemistry
State University of New York
at Stony Brook, Stony Brook
NY 11794-3400, USA

³Bristol-Myers Squibb
Pharmaceutical Research
Institute, PO Box 4000
Princeton, NJ 08543-4000
USA

⁴Graduate Program in
Biophysics and Graduate
Program in Molecular and
Cellular Biology, State
University of New York at
Stony Brook, Stony Brook
NY 11794, USA

The peripheral subunit-binding domain from the dihydrolipoamide acetyltransferase (E2) component of the pyruvate dehydrogenase multi-enzyme complex from *Bacillus stearothermophilus* is stably folded, despite its short sequence of only 43 amino acid residues. A 41 residue peptide derived from this domain, psbd41, undergoes a cooperative thermal unfolding transition with a t_m of 54°C. This three-helix protein is monomeric as judged by ultracentrifugation and concentration-dependent CD measurements. Peptides corresponding to the individual helices are largely unstructured both alone and in combination, indicating that the unusual stability of this protein does not arise solely from unusually stable α -helices. Chemical denaturation by guanidine hydrochloride is also cooperative with a ΔG_{H_2O} of 3.1 kcal mol⁻¹ at pH 8.0 and 25°C. The chemical denaturation is broad with an m -value of 760 cal mol⁻¹ M⁻¹. psbd41 contains a buried aspartate residue at position 34 that may provide stability and specificity to the fold. A mutant peptide, psbd41Asn was synthesized in which the buried aspartate residue was mutated to asparagine. This peptide still folds cooperatively and it is monomeric, but is much less thermostable than the wild-type with a t_m of only 31°C. Chemical denaturations at 4°C give an m -value of 740 cal mol⁻¹ M⁻¹, similar to the wild-type, but the stability ΔG_{H_2O} is only 1.4 kcal mol⁻¹. Both the wild-type and the mutant unfold at extremes of pH, but at 4°C psbd41Asn is folded over a narrower pH range than the wild-type. Although the mutant unfolds cooperatively by thermal and by chemical denaturation, its NMR spectrum is significantly broader than that of the wild-type and it binds ANS. These results show that Asp34 is vital for the stability and specificity of this structure, the second smallest natural sequence known to fold in the absence of disulfide bonds or metal or ligand-binding sites.

© 1998 Academic Press Limited

Keywords: protein folding; thermostability; pyruvate dehydrogenase multienzyme complex

*Corresponding author

Present addresses: R. Fairman, Department of Molecular, Cellular and Developmental Biology, Haverford College, Haverford, PA 19041, USA; J. A. Boice, Department of Biochemistry, Merck Research Laboratories, PO Box 2000 RY50-105, Rahway, NJ 07065, USA.

Abbreviations used: NOE, nuclear Overhauser effect; NOESY, nuclear Overhauser effect spectroscopy; DQF-COSY, double quantum filtered correlation spectroscopy; TOCSY, total correlation spectroscopy; t_m , midpoint of thermal denaturation transition; GdnHCl, guanidine hydrochloride; ΔASA , change in accessible surface area; ΔASA_{np} , change in non-polar accessible surface area; ΔASA_{pol} , change in polar accessible surface area; PAL, polystyrene Fmoc support for peptide amides; PAL-PEG-PS, polyethylene glycol polystyrene Fmoc support for peptide amides; TBTU, 2-(1H-benzotriazole-1-yl)-1,1,3,3-tetramethyluronium tetrafluoroborate; ANS, 1-anilinonaphthalene-8-sulfonate; Fmoc, N²-9-fluorenylmethyloxycarbonyl; ESI, electrospray ionization mass spectrometry; FAB, fast atom bombardment mass spectrometry; MALDI-TOF, matrix assisted laser desorption and ionization time of flight mass spectrometry; ppm, parts per million.

Introduction

Although there are a number of small to mid-sized peptides that are able to adopt significant helical structure in isolation, there are very few examples of small proteins of less than 60 residues that are able to adopt a stable tertiary structure. Until recently, the only small monomeric proteins known to fold with a unique tertiary structure contained either disulfide bonds, ligand-binding sites, metal coordination sites, or unnatural amino acids. Now, however, there are several known examples of small domains with amino acid sequences that are unremarkable but that acquire a stable tertiary fold (Alexander *et al.*, 1992; Bottomley *et al.*, 1994; Yu *et al.*, 1992; Kalia *et al.*, 1993; Clarke *et al.*, 1994; Wilkstrom *et al.*, 1994; Kraulis *et al.*, 1996; McKnight *et al.*, 1996, 1997; Dahiyat & Mayo, 1997). Of these, only three contain less than 50 amino acid residues (Kalia *et al.*, 1993; McKnight *et al.*, 1996, 1997; Dahiyat & Mayo, 1997). Such proteins offer interesting model systems for the study of protein folding. Their small size makes them ideal for computational approaches and makes them attractive targets for *de novo* design. Furthermore, it often means that they can be prepared by solid phase peptide synthesis, allowing the incorporation of unnatural amino acids. In addition, thermodynamic arguments suggest that they should be, at best, only marginally stable (Privalov, 1992). Thus, elucidating the interactions that stabilize these folds should contribute to our understanding of protein folding.

One such small protein is the peripheral subunit-binding domain of the dihydrolipoamide acetyltransferase component (E2) of the pyruvate dehydrogenase multienzyme complex from *Bacillus stearothermophilus*. This three-helix domain (Figure 1) was originally isolated from the larger structure by limited proteolysis (Duckworth *et al.*, 1982; Packman *et al.*, 1988). It comprises 43 amino acid residues, and its structure was solved by NMR (Kalia *et al.*, 1993). Its sequence is:

1	11	21	31	41
VIAMPSVRKY	AREKGVDIRL	VQGTGKNGRV	LKEDIDAFLA	GGA

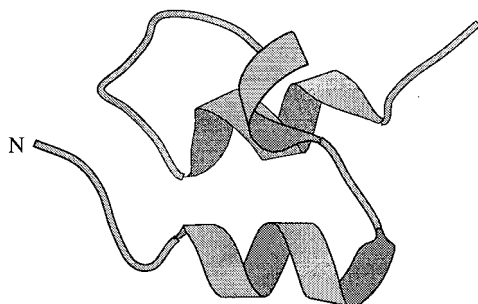


Figure 1. MOLSCRIPT figure (Kraulis, 1991) of the peripheral subunit-binding domain (Kalia *et al.*, 1993).

The domain contains a structured core of 33 amino acid residues comprising two parallel α -helices, Val7 to Lys14 and Lys32 to Leu39, connected by a loop that contains a short stretch of 3_{10} helix from Asp17 to Val21. The overall fold is very similar to the dimerization domain of the E3 subunit (dihydrolipoamide dehydrogenase) of the pyruvate dehydrogenase multienzyme complex from *Azobacter vinelandii* (Brocklehurst *et al.*, 1994). The loop remains structured and packs against the two helices as a result of a novel hydrogen bonding network involving the buried, charged Asp34 side-chain and the backbone amide groups of Gly23, Thr24, Gly25 and Leu31 as well as the side-chain hydroxyl group of Thr24. Furthermore, the NMR data show many slowly exchanging amide protons, providing additional evidence for a unique, stably folded structure. No long-range NOEs were observed from the N-terminal six residues or from the C-terminal four residues, suggesting that only a 33 residue core from Val7-Leu39 is structured; however, Ala40, Gly41 and Gly42 all show some protection from hydrogen-deuterium exchange, indicating that they participate in some sort of structure, and the segment from Met4 to Ser6 appears to adopt a right-handed helical conformation (Kalia *et al.*, 1993). These studies have established the structure of this domain but it is not known whether the peripheral subunit-binding domain unfolds cooperatively, nor has the role of the buried aspartate residue been investigated.

Here, we show that a 41 residue peptide derived from the peripheral subunit-binding domain undergoes cooperative folding transitions. Peptides corresponding to each of the helices are largely unstructured, both alone and in combination, suggesting that this unusually small domain is not stabilized simply by a sequence of high helix-forming propensity. Although a mutant in which the buried aspartic acid side-chain is replaced by asparagine also folds cooperatively, it shows much lower thermal and chemical stability than the wild-type and has a narrower pH range in which it is stable, indicating an important role for the buried

aspartate residue in stabilizing and specifying the tertiary fold.

Results and Discussion

A 41 residue peptide, psbd41, corresponding to the sequence Ala3 to Gly43 of the peripheral subunit-binding domain was synthesized. Figure 2A shows the far-UV circular dichroism (CD) spectrum of psbd41 at pH 7.1. This peptide is 33% helical, based on mean residue ellipticity at 222 nm (Figure 2A). Considering only α -helical residues and not those in the 3_{10} helix, the expected value is

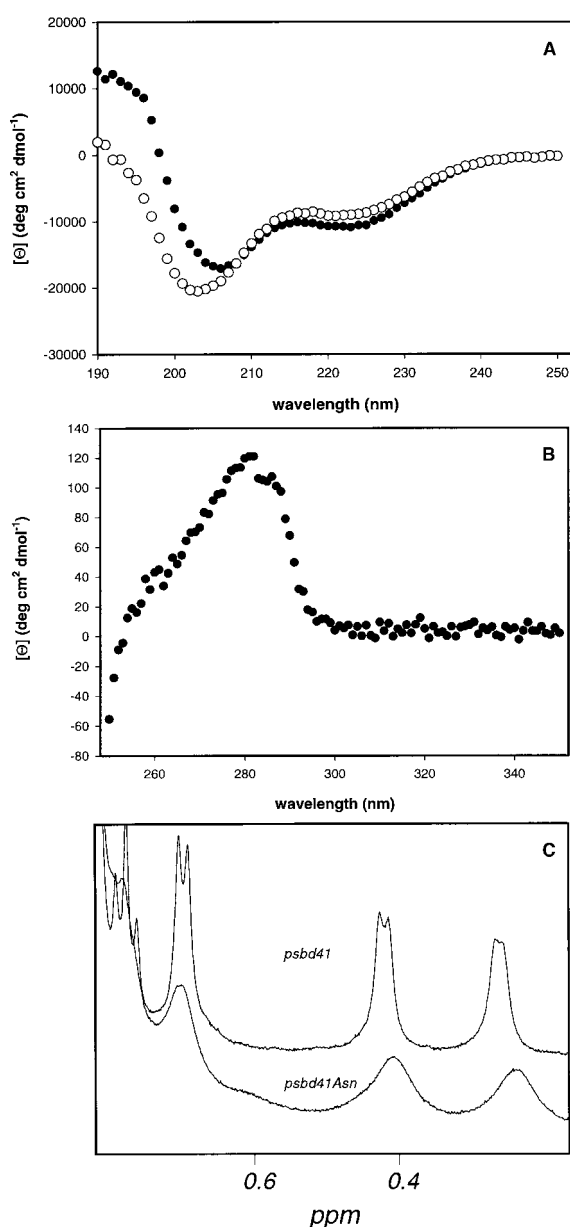


Figure 2. A, Far-UV CD spectra of 403 μM psbd41 at 25°C (filled circles) and 46.6 μM psbd41Asn at 4°C (open circles). The spectra were recorded in 2 mM sodium phosphate, 2 mM sodium citrate, 2 mM sodium borate, 50 mM NaCl (pH 7). B, Near-UV CD spectrum of 77.5 μM psbd41 in 2 mM sodium phosphate, 2 mM sodium citrate, 2 mM sodium borate, 50 mM NaCl (pH 8) at 25°C. C, One-dimensional proton NMR spectra of psbd41 at 25°C (top) and psbd41Asn at 4°C (bottom).

39% helix. Observed helicities calculated from CD do not always match the values predicted from the structures because, for several reasons, CD spectra can be difficult to interpret. First, the rotational strength of the transitions that contribute to the helical bands is strongly dependent on local backbone geometry, the length of the helices, and the presence or absence of aromatic residues (Manning & Woody, 1991; Woody, 1978; Chakrabarty *et al.*,

1993). In addition, the CD spectrum of 3_{10} helices is not completely understood (Manning & Woody, 1991). These caveats regarding the interpretation of CD spectra suggest that the discrepancies between helical contents observed by CD and those calculated from NMR or X-ray crystal structures are intrinsic to CD spectroscopy and do not necessarily arise from differences in structure. psbd41 shows far-UV CD characteristic of a helical peptide with a double minimum at 222 and 208 nm (Figure 2A), and it has a positive band with a maximum at about 280 nm in the near-UV, indicating that the sole tyrosine residue (Tyr10) is in an asymmetric environment (Figure 2B). A near-UV CD signal is often taken as evidence for the formation of a tightly packed hydrophobic core typical of a compact, folded structure rather than a molten globule-like structure. Ring current shifted methyl resonances observed in the one-dimensional proton NMR spectrum (top spectrum, Figure 2C) also provide evidence of a well-packed hydrophobic core. Furthermore, NMR spectra of psbd41 (NOESY, DQF-COSY and TOCSY, data not shown) indicate that most residues have chemical shifts nearly identical with those reported by Kalia *et al.* (1993), suggesting that it adopts the same structure as the full-length 43 residue peripheral subunit-binding domain. The spectra were taken under different conditions (295 K, pH 5.0 for the studies by Kalia *et al.* (1993) compared with 288 K, pH 5.3 in this study), so slight differences are not unexpected. Except near the N terminus, very few resonances differ by more than 0.12 ppm. The chemical shifts of protons in the N-terminal five residues differ between 0.22 and 0.26 ppm relative to the values reported by Kalia *et al.* (1993). These larger differences near the N terminus may be due to the absence of two residues in psbd41 relative to the complete peripheral subunit-binding domain.

Many small protein domains are known to oligomerize, and in the pyruvate dehydrogenase multi-enzyme complex from *A. vinelandii* there is a dimerization interface that has a topology similar to that of the domain studied here (Brocklehurst *et al.*, 1994). Hence, it is important to establish that psbd41 is monomeric under the conditions of the experiments reported here. Analytical ultracentrifugation experiments on a 234 μM sample show that psbd41 is monomeric. The data were fit using an ideal single-species model with the molecular mass treated as an adjustable parameter (Figure 3). The apparent molecular mass of 4450(\pm 160) Da is in good agreement with the true value of 4430 Da. In addition, the mean residue ellipticity at 222 nm is independent of concentration over the measured range of 130 μM to 3.05 mM (data not shown). Thus, unlike its structural analog from the E3 subunit, psbd41 is monomeric over the concentration range used in these studies.

One reason that such a small structure might be folded is if the individual helices are particularly stable. To address this possibility, two peptides corresponding to the first helix (denoted helix

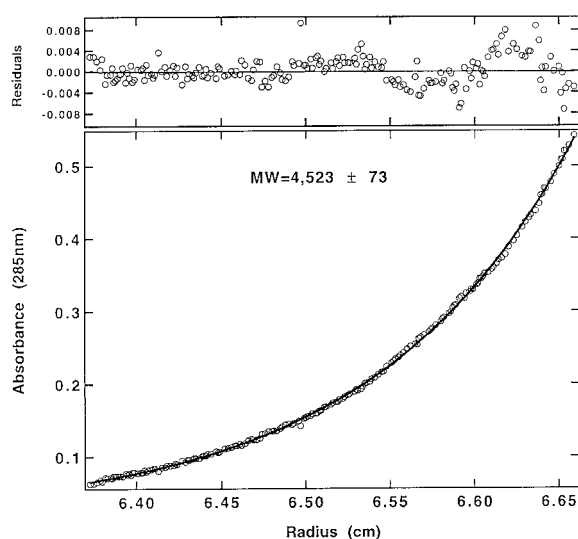


Figure 3. Analytical ultracentrifugation of psbd41 shows that it is monomeric. The absorbance at 288 nm is plotted *versus* radial distance for a rotor speed of 50,000 rpm. The data were fit to a single species allowing the molecular mass to float. The apparent molecular mass of 4450(\pm 160) Da is in good agreement with the true molecular mass of 4430 Da. The residuals, shown above the absorbance *versus* radial distance plot, are random.

1(P5-V16) and helix 1(A3-V16) with residue numbers corresponding to positions in the full-length 43 residue domain) and a third corresponding to the second helix (helix 2 (Leu31-Ala43)) were synthesized. The Chou & Fasman (1978) secondary structure prediction program predicts that residues 3 to 15 and 28 to 41 will be helical, but according to several helix-forming propensity scales (O'Neil & DeGrado, 1990; Wojcik *et al.*, 1990), the residues in the helices have only a moderate propensity to adopt a helical structure. In addition, AGADIR (Munoz & Serrano, 1994, 1995a,b) predicts a very low helix content. As judged by CD, helix 1(P5-V16) and helix 2 were largely unstructured at 25°C and at 4°C over the pH range of 2 to 12. At pH 7 and 25°C, the estimated helix content of helix 1(P5-V16) is less than 12%, while that for helix 1(A3-V16) is less than 11% using the equations given by Rohl & Baldwin (1997). The estimated helix content for helix 2 is less than 20% using the same equations. There is no change in the helical content when the two peptides are mixed. The spectrum obtained from a mixture of helix 1(P5-V16) and helix 2 was equal to the sum of the spectra of the individual peptides (Figure 4). Differences at the lowest wavelengths are most likely the result of either light-scattering or absorbance artifacts due to the higher peptide concentration in the solution containing both peptides. The same result was observed for a mixture of helix 1(A3-V16) and helix 2. Thus the unusual stability of the peripheral subunit-binding domain can not be due entirely to a high intrinsic stability of the isolated helices.

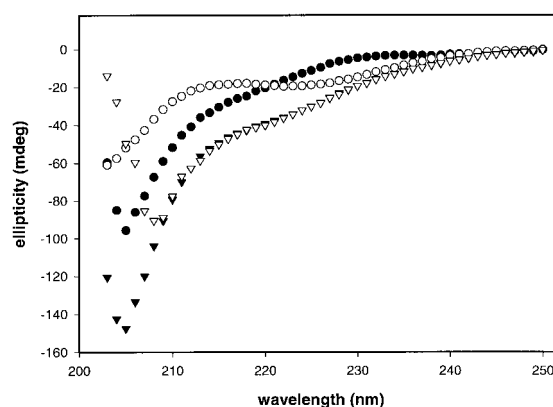


Figure 4. Far-UV CD spectra of helix 1(P5-V16) and helix 2, alone and in combination. Filled circles, a 538 μ M sample of helix 1(P5-V16). Open circles, a 238 μ M sample of helix 2. Filled triangles, mathematical sum of the spectra of helix 1(P5-V16) and helix 2. Open triangles, spectrum of a solution containing both 538 μ M helix 1(P5-V16) plus 238 μ M helix 2. All spectra were recorded at 25°C in 2 mM sodium phosphate, 2 mM sodium borate, 2 mM sodium citrate, 20 mM NaCl (pH 7).

Thermal and chemical denaturations of psbd41 were performed in order to study the equilibrium thermodynamics of folding. Thermal denaturations were monitored by both near and far-UV CD at a variety of pH values and by one-dimensional proton NMR at an apparent pH of 8 (Figure 5A). Values of t_m and ΔH were extracted from the melting curves by non-linear least-squares fitting of the data to the equation reported by Tan *et al.* (1995). Thermal unfolding is greater than 98% reversible at ionic strengths of 50 mM (NaCl) or higher. Thermal denaturations could also be followed with NMR because the protein unfolds in the fast to intermediate exchange regime. Plotting the fraction unfolded *versus* temperature for denaturations at pH 8 monitored by near and far-UV CD and for apparent pH 8 monitored by NMR results in coincident curves (Figure 5A), each with a t_m value of 54°C, suggesting that thermal unfolding is a two-state process. The t_m values for the protein in $^2\text{H}_2\text{O}$ measured by near and far-UV CD are identical with those measured in H_2O . The slight deviation in the low-temperature baseline on the curves of fraction unfolded *versus* temperature is a result of the difficulty in fitting the pretransition region of the data. In addition, although the transition regions essentially overlay, the NMR data in the post-transition region are not a perfect match with those from CD. Due to limits of the NMR probe it was not possible to obtain post-transition data at higher temperatures, making it difficult to fit the post-transition region of the NMR data accurately. Despite these difficulties, t_m values can be measured reliably because they are the points of inflection in the transition region.

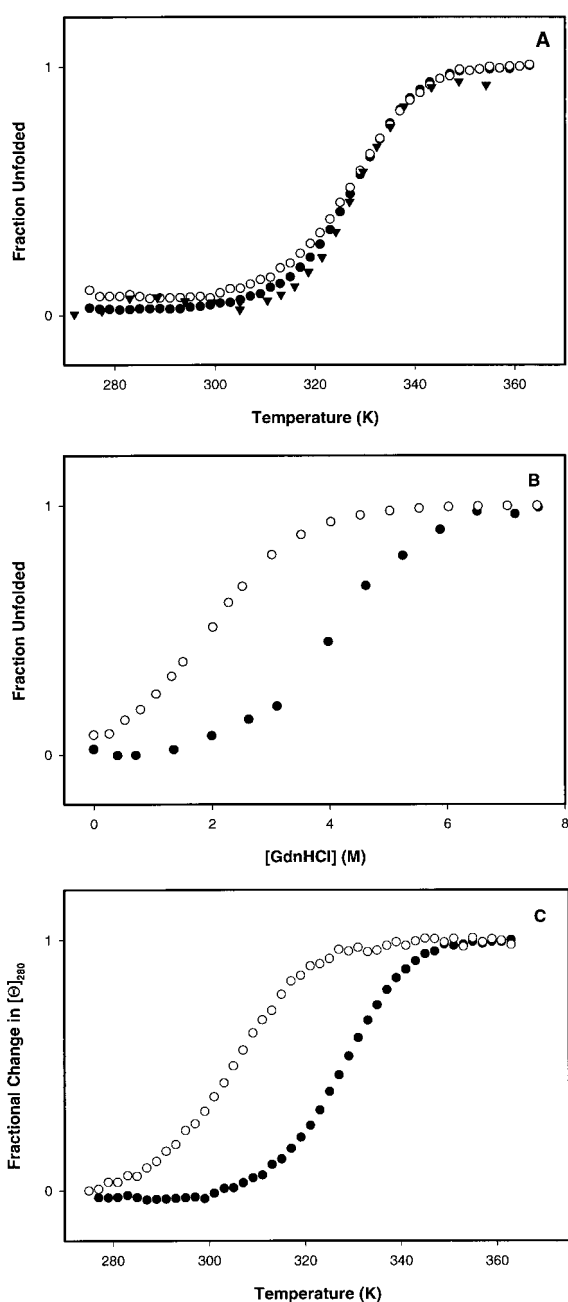


Figure 5. A, Thermal denaturation of psbd41 at pH 8.0. Filled circles, near-UV CD (280 nm) of 915 μM psbd41. Open circles, far-UV CD (222 nm) of 61 μM psbd41. Filled triangles, NMR – chemical shift of Tyr10 C^δ proton. Data are normalized to fraction unfolded. B, Denaturation by GdnHCl of 121 μM psbd41 (filled circles) and 83 μM psbd41Asn (open circles). Denaturation was monitored by far-UV CD at 222 nm in a 1 mm cuvette at 25°C for psbd41 and at 4°C for psbd41Asn. C, Thermal denaturation of 915 μM psbd41 (filled circles) and 614 μM psbd41Asn (open circles) monitored by near-UV CD at 280 nm. Data are normalized to fraction of maximal change in ellipticity.

et al., 1995; Pace *et al.*, 1990), and as low as 0.3 kcal mol⁻¹ K⁻¹, the value calculated based on change in accessible surface area (Myers *et al.*, 1995). Both the t_m and the ΔH values extracted from the curve fit were insensitive to the value of ΔC_p used. The t_m value obtained from the curve fits is identical for all three techniques, but ΔH is very sensitive to the way the pre-transition region is defined. The values of ΔH obtained from the various spectroscopic techniques range from 26 to 42 kcal mol⁻¹. Although this is a wide range, these values of ΔH are within the normal range expected for globular proteins on a per residue basis (Privalov & Gill, 1988).

In principle, ΔC_p can be determined to a high degree of accuracy by measuring ΔH as a function of temperature. Typically, changes in pH are used to alter the t_m , and ΔH at the midpoint is extracted by fitting the thermal denaturation curves using the Gibbs-Helmholtz equation. However, psbd41 has no group that titrates between pH 4.8 and pH 9, so the t_m value is nearly independent of pH. The narrow range of this parameter precludes the accurate determination of ΔC_p .

Chemical denaturations were also monitored by far-UV CD. At 25°C, the unfolding transition induced by guanidine hydrochloride (GdnHCl) is greater than 98% reversible, and is broad but cooperative (Figure 5B). The m -value for denaturation by GdnHCl is 760(\pm 130) cal mol⁻¹ M⁻¹. Extrapolation to 0 M GdnHCl provides an estimated stability in water of 3.1(\pm 0.5) kcal mol⁻¹.

The m -value of chemical denaturation is an indication of the change in accessible surface area (ΔASA) between the native and denatured states (Tanford, 1970). For a small protein, one would expect a small ΔASA value, and therefore a small m -value and a broad unfolding transition. Using the ACCESS routine from the WHAT IF software package (EMBL, Heidelberg, Germany; Vriend, 1990) and the distinction that N and O atoms are polar and all other atoms are non-polar (Spolar *et al.*, 1992), $\Delta\text{ASA}_{\text{pol}} = 1121 \text{ \AA}^2$ and $\Delta\text{ASA}_{\text{np}} = 1532 \text{ \AA}^2$ between the native conformation and an extended β -conformation. From these values, an m -value of 836 cal mol⁻¹ M⁻¹ is calculated using the equation provided by Myers *et al.* (1995). This calculated value is within the error of the curve fit to the data from which the experimental value was determined. The small net change in accessible surface area accounts for the broad chemical denaturation transition.

Buried charges are rare in proteins because the desolvation of a charge is extremely unfavorable. When they occur, the charge is usually involved in a salt-bridge, or occasionally in a hydrogen bonding network, and is usually important either to structure or function. Since Asp34 is buried, its function cannot be in peripheral subunit binding, and so its role must be structural. In addition to the hydrogen bonding network, the charge may be stabilized by favorable interactions with the macrodipole of helix 2. Buried polar residues have been

Curve fits were repeated using ΔC_p values as high as 0.645 kcal mol⁻¹ K⁻¹, the value predicted empirically for the full 43 residue domain (Tan

shown to play a role in the specificity of structure formation (Betz *et al.*, 1993; Hendsch & Tidor, 1994; Nobbs *et al.*, 1994; Lumb & Kim, 1995; Raleigh *et al.*, 1995; Schueler & Margalit, 1995; Gonzalez *et al.*, 1996), perhaps by preventing the formation of alternative structures.

To investigate the role of the buried aspartic acid residue, a mutant peptide was synthesized in which Asp34 was replaced with an asparagine residue (psbd41Asn). Analytical ultracentrifugation shows that the peptide is monomeric at 142 μM . In addition, the t_m measured for psbd41Asn is independent of concentration from 36 μM to 614 μM , suggesting that the peptide remains monomeric within this concentration range. By far-UV CD, at pH 7.0 and 25°C, this peptide is less structured than the wild-type, with a CD signal at 222 nm corresponding to 23% helix content. Upon lowering the temperature to 4°C, the helical content increases to 26% (Figure 2A) and psbd41Asn develops a near-UV CD signal closer to that of the wild-type.

Thermal denaturations show that psbd41Asn folds cooperatively, but it has a significantly lower t_m than that of psbd41, with a value of 31°C compared to 54°C for the wild-type (Figure 5C). Denaturations by GdnHCl provide further evidence that the asparagine mutation is destabilizing (Figure 5B). The denaturation was performed at 4°C because psbd41Asn is partially unfolded at 25°C. Denaturations by GdnHCl are 90% reversible, and the m -value of denaturation is 740 cal mol⁻¹ M⁻¹, which is very similar to the value for the wild-type, 760 cal mol⁻¹ M⁻¹. However, the midpoint is only 1.9 M GdnHCl for psbd41Asn and the stability $\Delta G_{\text{H}_2\text{O}}$ is 1.4 kcal mol⁻¹. Ideally, the stability of the mutant should be compared to that of the wild-type at the same temperature, but even at 10°C there was insufficient post-transition data for the wild-type to determine a $\Delta G_{\text{H}_2\text{O}}$ value. The midpoint for the wild-type at this temperature is at least 5 M GdnHCl. At 25°C, the stability of psbd41 is 3.1 kcal mol⁻¹ and the midpoint is 4.1 M GdnHCl.

One-dimensional proton NMR spectra of psbd41Asn at 4°C indicate the presence of ring current shifted methyl resonances, as observed for the wild-type sequence; however, the majority of resonances in the spectrum are much broader than expected for a monomeric protein that folds into a unique structure. For example, the linewidth of the most upfield shifted methyl resonance is two to three times broader for the mutant protein than for the wild-type and, unlike the wild-type, the J -coupling is no longer resolved (bottom spectrum, Figure 2C). Spectra of the mutant were recorded at concentrations of 300 μM and 3 mM and were identical, so it is highly unlikely that the increased linewidth is due to aggregation.

The increased linewidth is reminiscent of the spectra observed for proteins in the molten globule state or for some designed proteins that are known to have flexible, loosely packed hydrophobic cores.

In these cases, the increase in linewidth is considered to be due to intermediate exchange behavior occurring on the millisecond timescale or faster (Baum *et al.*, 1989), although there may be a contribution to the observed linewidths due to exchange between the folded and unfolded conformations. The NMR study suggests that there is some conformational flexibility in psbd41Asn. Titrations with 1-anilinonaphthalene-8-sulfonate (ANS) were performed to determine whether it would bind to psbd41Asn. ANS binds to hydrophobic surfaces on molten globules, but it does not bind to unfolded or, with few exceptions, to native proteins. When it binds, its fluorescence quantum yield increases, and the emission maximum shifts from 515 nm for free ANS in water to near 490 nm. Unlike the wild-type sequence, psbd41Asn appears to bind ANS. The fluorescence emission maximum shifts from 515 nm to 490 nm, and the fluorescence intensity increases fivefold. In contrast, no change is observed in the emission maximum for the wild-type, and the fluorescence intensity increases only slightly.

Since psbd41Asn has a near-UV CD signal and ring current shifted methyl resonances, it does not possess all the characteristics typical of a classic molten globule (Kuwajima, 1989); rather, it resembles more closely the structured molten globules (Morozova *et al.*, 1995; Ptitsyn, 1996; Kay & Baldwin, 1996). It is possible that psbd41Asn is less stable than the wild-type sequence because the asparagine side-chain is slightly larger than that of aspartate and it cannot be accommodated in the core of the structure, but a more likely explanation is that asparagine cannot participate properly in the hydrogen bonding network.

pH titrations also highlight the potential role of Asp34 in specifying the tertiary fold. The wild-type protein, psbd41, unfolds at extremes of pH. pH titrations were monitored by both near and far-UV CD at 25°C, and the signal changes sigmoidally with pH. Plots of fraction unfolded *versus* pH are coincident, suggesting that pH-induced unfolding is a two-state process. The protein begins to unfold below pH 5.3, and the transition is complete by pH 2.5. The midpoint is approximately pH 3.4, which is about 0.5 pK_a unit lower than is typical for an aspartic or glutamic acid side-chain. The protein also begins to unfold above pH 10, most likely due to the deprotonation of lysine, tyrosine and possibly arginine residues. Since psbd41Asn is not fully folded at 25°C, its pH behavior was compared to that of the wild-type at a lower temperature. At 4°C, the wild-type protein becomes slightly more stable to extremes of pH, unfolding above pH 11 and below pH 4 with a midpoint of approximately 2.9. The transition is not complete until pH 2 (Figure 6). There are several reasons why psbd41 might unfold at acidic and basic pH values. Charge repulsion may play a role at extremes of pH. Protonation of the acidic residues would lead to a large positive charge on the pro-

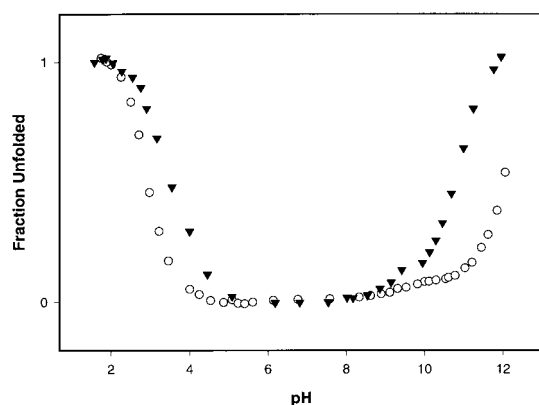


Figure 6. pH titrations of psbd41 and psbd41Asn at 4°C monitoring far-UV CD at 222 nm. Open circles, 20.6 μ M psbd41. Filled triangles, 15.4 μ M psbd41Asn.

tein, and likewise the deprotonation of the basic residues and the single tyrosine residue results in a large negative charge. Loss of favorable local electrostatic interactions may also destabilize the protein at extremes of pH (Lyu *et al.*, 1992; Scholtz *et al.*, 1993). Unfolding at low pH may also be caused by the protonation of Asp34, which would disrupt the hydrogen bonding network, as does the psbd41Asn mutant, destabilizing the structure.

psbd41Asn also unfolds at extremes of pH, but the range through which it is stable is narrower than that for psbd41. At 4°C, the protein begins to unfold above pH 9 and, unlike the wild-type, the transition is nearly complete by pH 12. At acidic pH values, psbd41Asn begins to unfold below pH 5, with a midpoint of about 3.5, and the transition is complete by pH 2 (Figure 6). The fact that psbd41Asn is destabilized at both low and high values relative to psbd41 suggests that Asp34 is very important to the stability of the peripheral subunit-binding domain.

Conclusions

The cooperative unfolding transitions of psbd41 are in contrast to those of many small, folded peptides and proteins that unfold with diffuse thermal and chemical transitions. For example BBA1, a 23 residue β , β , α domain that was designed on the basis of the zinc finger folding motif, folds independently of zinc but contains a D-proline residue and the non-natural amino acid 2-(1,10-phenanthroline-2-yl)-L-alanine and has diffuse thermal and chemical denaturations (Struthers *et al.*, 1996). Another recently designed structure was based on the Z-domain of protein A, a three-helix bundle. Since only two of the helices are involved in binding to immunoglobulin G, the third helix was removed and the sequence was altered to stabilize the smaller domain. The resulting 38 residue peptide was helical and bound IgG with only fourfold lower affinity than the original 59 residue protein

(Braisted & Wells, 1996), but is not fully folded even at low temperature. To increase the stability, several changes were made to the sequence, including the addition of a disulfide bond (Starovasnik *et al.*, 1997).

There is only one other example of such a small natural protein that displays cooperative unfolding transitions in the absence of disulfide bonds or metal binding. McKnight *et al.* (1996) report the thermodynamic characterization of another small domain, HP-35, which was obtained by limited proteolysis of the actin-binding protein villin. A recent NMR structure shows that this 35 residue peptide is also a three-helix protein, but with topology very different from that of the peripheral subunit-binding domain (McKnight *et al.*, 1997). Like psbd41, it shows cooperative thermal denaturation and chemical denaturation transitions. It is more thermostable than the peripheral subunit-binding domain, with a t_m of 70°C, but chemical denaturation by GdnHCl gave similar stability and m -values. HP-35 has a ΔG_{H_2O} of 3.3 kcal mol⁻¹ and an m -value of 800 cal mol⁻¹ M⁻¹ at 4°C (McKnight *et al.*, 1996), compared to 3.1 kcal mol⁻¹ and 760 cal mol⁻¹ M⁻¹ for psbd41 at 25°C. High t_m values are commonly seen for small proteins, even with low chemical stabilities (Alexander *et al.*, 1992).

We have shown that the peripheral subunit-binding domain of the dihydrolipoamide acetyltransferase component from the pyruvate dehydrogenase multienzyme complex undergoes cooperative folding transitions. psbd41 is monomeric up to at least 3.05 mM, and has a stability in water, ΔG_{H_2O} , of 3.1 kcal mol⁻¹ and is reasonably thermostable with a t_m of 54°C. Though not an extraordinarily stable structure, it is nevertheless impressive that such a small protein is folded. In addition, it appears that the buried aspartic acid residue is vital for the specificity of structure formation and for the stability of this protein. This small structure offers an attractive target for *de novo* design efforts and provides a useful model system with which to study both thermodynamics and kinetics of protein folding.

Materials and Methods

Materials

PAL and PAL-PEG-PS resins were purchased from Perceptive Biosystems (Framingham, MA). TBTU was purchased from Advanced Chemtech (Louisville, KY). Fmoc-protected amino acids were purchased from both of these companies. ANS was purchased from Molecular Probes (Eugene, OR). All other solvents and reagents were from Fisher Scientific (Springfield, NJ).

Peptide synthesis and purification

Peptides were prepared by solid phase synthesis using a Millipore 9050 Plus or Rainin PS-3 automated peptide synthesizer and standard Fmoc chemistry. Five peptides were synthesized. psbd41 corresponds to resi-

dues Ala3 to Ala43 of the peripheral subunit-binding domain. psbd41Asn has the same sequence as psbd41, except for the mutation of Asp34 to Asn. Helix 1(P5-V16) corresponds to residues Pro5 through Val16, helix 1(A3-V16) is Ala3 through Val16, and helix 2 is residues Leu31 through Ala43. All peptides had acetylated N termini and amidated C termini. Residue numbers correspond to positions in the full-length peripheral subunit-binding domain. All peptides were purified by HPLC on a C18 reverse phase column (Vydac). psbd41Asn, helix 1(P5-V16), helix 1(A3-V16) and helix 2 were purified using a water/acetonitrile gradient containing 0.1% (v/v) trifluoroacetic acid. psbd41 was purified using first a water/acetonitrile gradient containing 170 mM triethylamine phosphate (pH 2.5 to 3.0) followed by a second step using a water/acetonitrile gradient containing 0.1% trifluoroacetic acid. Peptides were greater than 95% pure. Peptide identity was confirmed by mass spectrometry. Electrospray ionization (ESI) mass spectrometry gave a molecular mass of 4429.0 Da for psbd41 (expected 4430) and 1632.6 Da for helix 1(A3-V16) (expected 1631). Fast atomic bombardment mass spectrometry (FAB) was used to determine a molecular mass of 4428.7 Da for psbd41Asn (expected 4428.2) and 1430.8 Da for helix 1(P5-V16) (expected 1430.6). Finally, helix 2 had a molecular mass of 1362.4 Da as determined by matrix assisted laser desorption and ionization time of flight (MALDI-TOF) mass spectrometry (expected 1361.5).

Circular dichroism

All CD experiments in this work were performed on an Aviv 62A DS CD spectrophotometer in a buffer of 2 mM sodium phosphate, 2 mM sodium borate, 2 mM sodium citrate containing 50 mM NaCl for psbd41 and psbd41Asn or 20 mM NaCl for helix 1(P5-V16), helix 1(A3-V16) and helix 2. Far-UV CD spectra are the average of five repeats in a 0.1 mm cuvette. Near-UV CD spectra are the average of ten repeats in a 1 cm cuvette. Except for helix 2, all peptide concentrations for all experiments were determined by UV spectroscopy, measuring the absorbance at 276 nm in 6 M GdnHCl, 20 mM NaH₂PO₄ using an extinction coefficient of 1420 M⁻¹ cm⁻¹. Since helix 2 contains no tyrosine or tryptophan, its concentration was determined by amino acid analysis performed in triplicate. Fraction helix was calculated based on the molar ellipticity at 222 nm using the equations given by Rohl & Baldwin (1997). pH titrations were monitored by far-UV CD at 222 nm and were performed by the addition of HCl to the sample in a stirred 1 cm cuvette at either 25° or 4°C. The concentration dependence of the CD of psbd41 was monitored at 25°C. The mean residue ellipticity was measured at 222 nm for peptide concentrations of 130 μM to 3.05 mM at pH 8.0 and found to be independent of concentration.

One-dimensional proton nuclear magnetic resonance

One-dimensional spectra of 4 mM psbd41 and 3 mM psbd41Asn were acquired with a Varian Instruments Inova 500 MHz nuclear magnetic resonance spectrometer using standard presaturation for water suppression. The peptides were dissolved in 90% H₂O/10% ²H₂O with 150 mM tetramethylsilylpropionate as a chemical shift standard. Spectra of 3.5 mM psbd41 in

20 mM deuterated Tris in ²H₂O (apparent pH 8.0, uncorrected pH meter reading) to monitor thermal denaturation were measured on a Bruker AMX-600 using standard presaturation for water suppression.

Analytical ultracentrifugation

Analytical ultracentrifugation was performed to test whether psbd41 and psbd41Asn are monomeric. Experiments were performed at 25°C with a Beckman XL-A analytical ultracentrifuge using a rotor speed of 50,000 rpm; 12 mm pathlength, six-channel, charcoal-filled Epon cells with quartz windows were used. Ten scans were averaged. Partial specific volumes were calculated from the weighted average of the partial specific volumes of the individual amino acids (Cohn & Edsall, 1943). The HID program from the Analytical Ultracentrifugation Facility at the University of Connecticut was used for data analysis, and equilibrium sedimentation analysis software running under Igor (Wavemetrics, Lake Oswego, OR) using the algorithm given by Johnson *et al.* (1981) was used for preparation of the figures. The psbd41 sample was dialyzed against 10 mM sodium phosphate, 100 mM NaCl (pH 7.3), while the psbd41Asn sample was dissolved in 2 mM sodium phosphate, 2 mM sodium borate, 2 mM sodium citrate, 50 mM NaCl (pH 8.0) and was not dialyzed.

Analysis of unfolding curves

Thermal denaturations were performed at pH 8.0 and monitored by far-UV CD (222 nm) or near-UV CD (280 nm), or NMR, following the chemical shift of the C^δ proton of Tyr10 at 7.08 ppm. For CD experiments, peptides were dissolved in 2 mM sodium phosphate, 2 mM sodium borate, 2 mM sodium citrate, 50 mM NaCl, and temperature was raised from 2° to 90°C by 2°C intervals. CD was measured in a 5 mm cuvette, which was allowed to equilibrate at each temperature for four minutes, and the signal was averaged for 60 seconds. CD experiments were repeated in ²H₂O. Reversibility was ascertained by comparing the ellipticity at 2°C after a thermal denaturation to the initial ellipticity at 2°C. Thermal denaturations of psbd41 were greater than 98% reversible and those of psbd41Asn were greater than 90% reversible. NMR spectra of 3.5 mM psbd41 in 20 mM deuterated Tris in ²H₂O (apparent pH 8) were acquired at 5 deg. C intervals in the pre- and post-transition regions (2 to 37°C, 62 to 77°C) and at 2.5°C intervals in the transition region (37 to 62°C). The probe temperature was calibrated with methanol between 2 and 22°C, and with ethylene glycol between 32 and 72°C (Raiford *et al.*, 1979). NMR data were analyzed using Felix (BIOSYM Technologies) running on an Iris workstation. All thermal denaturations were analyzed by non-linear least-squares curve fitting using SigmaPlot (Jandel Scientific) and the equations reported by Tan *et al.* (1995) after correction for the typographical error of a factor of *RT*. Data are normalized to fraction unfolded or fractional change in ellipticity.

Denaturations with GdnHCl were monitored by far-UV CD at 222 nm in a 1 mm cuvette at 25°C for 121 μM psbd41 and 4°C for 83 μM psbd41Asn. Samples were prepared by mixing the same volume of peptide with varying ratios of buffer (2 mM sodium phosphate (pH 8), 2 mM sodium borate, 2 mM sodium citrate, 50 mM NaCl) and GdnHCl in the same buffer

to give a constant peptide concentration and varying GdnHCl concentrations. GdnHCl concentration was measured by change in refractive index, using the equation (Pace *et al.*, 1990):

$$[\text{GdnHCl}] = 57.147(\Delta n) + 38.68(\Delta n)^2 - 91.60(\Delta n)^3$$

Reversibility was ascertained by comparing the far-UV CD spectrum of a sample prepared at a low concentration of GdnHCl to one first prepared in a high concentration of GdnHCl, incubated overnight, and then diluted to the low concentration of GdnHCl. Denaturations of psbd41 were greater than 98% reversible, and those for psbd41Asn were greater than 90% reversible. Data were analyzed by non-linear least-squares curve fitting using SigmaPlot (Jandel Scientific). Experimentally determined *m*-values were compared to those determined theoretically from the data reported by Myers *et al.* (1995) based on change in accessible surface area. The accessible surface area of the folded state was determined using the program WHAT IF (EMBL, Heidelberg, Germany; Vriend, 1990) to analyze the best representative structure from the ensemble of NMR-derived structures. The structure was identified using the program NMRCCLUS by Kelley *et al.* (1996).

ANS titrations

psbd41Asn was dissolved in 2 mM sodium citrate, 2 mM sodium borate, 2 mM sodium phosphate (pH 7.3), 50 mM NaCl to 1.37 mM. ANS was dissolved in methanol, and its concentration was measured using an extinction coefficient of $6800 \text{ M}^{-1} \text{ cm}^{-1}$ at 370 nm. An aliquot of ANS was diluted in the phosphate buffer to achieve a concentration of 10 μM ANS. This sample was titrated with psbd41Asn, and fluorescence was measured at 5°C for protein concentrations ranging from 0 to 101.4 μM . The sample was excited at 370 nm and the emission spectrum was measured from 400 nm to 600 nm. The experiment was repeated, titrating with a 627 μM sample of psbd41 to achieve protein concentrations ranging from 0 to 46 μM and measuring ANS fluorescence at 25°C.

Acknowledgments

We thank Professor N. Sampson for helpful discussions. We thank Dr Paul Young for acquiring one-dimensional NMR spectra of psbd41Asn. We thank Mr Daniel Moriarty for collecting the MALDI-TOF mass spectra at the Center for the Analysis of the Structure of Biological Macromolecules at the State University of New York at Stony Brook. All other mass spectrometry was performed at the University of Illinois Mass Spectrometry Center. We thank Preston Hensley for the equilibrium sedimentation analysis software (Smith Kline Beecham, King of Prussia, PA). Amino acid analysis was performed by Commonwealth Biotechnologies, Inc. The NMR facility at SUNY Stony Brook is supported by grants from the NSF (CHE8911350, CHE9413510) and from the NIH (1S10RR554701). This work was supported by NIH grant R29GM544233 to D.P.R., who is a Pew Scholar in the Biomedical Sciences. S.S. was supported in part by a Graduate Council Fellowship from the Office of Graduate Studies at the State University of New York at Stony Brook.

B.K. was supported in part by a GAANN fellowship from the Department of Education.

References

- Alexander, P., Fahnestock, S., Lee, T., Orban, J. & Bryan, P. (1992). Thermodynamic analysis of the folding of the streptococcal protein G IgG-binding domains B1 and B2: why small proteins tend to have high denaturation temperatures. *Biochemistry*, **31**, 3597–3603.
- Baum, J., Dobson, C. M., Evans, P. E. & Hanley, C. (1989). Characterization of a partly folded protein state by NMR methods: studies on the molten globule state of guinea pig α -lactalbumin. *Biochemistry*, **28**, 7–13.
- Betz, S. F., Raleigh, D. P. & DeGrado, W. F. (1993). *De novo* protein design: from molten globules to native like states. *Curr. Opin. Struct. Biol.* **3**, 601–610.
- Bottomley, S. P., Popplewell, A. G., Scawen, M., Wan, T., Sutton, B. J. & Gore, M. G. (1994). The stability and unfolding of an IgG binding protein based upon the B domain of protein A from *Staphylococcus aureus* probed by tryptophan substitution and fluorescence spectroscopy. *Protein Eng.* **7**, 1463–1470.
- Braisted, A. C. & Wells, J. A. (1996). Minimizing a binding domain from protein A. *Proc. Natl Acad. Sci. USA*, **93**, 5688–5692.
- Brocklehurst, S. M., Kalia, Y. N. & Perham, R. N. (1994). Protein-protein recognition mediated by a mini-protein domain: possible evolutionary significance. *Trends Biochem. Sci.* **19**, 360–361.
- Chakrabartty, A., Kortemme, T., Padmanabhan, S. & Baldwin, R. L. (1993). Aromatic side-chain contribution to far-ultraviolet circular dichroism of helical peptides and its effect on measurement of helix propensities. *Biochemistry*, **32**, 5560–5565.
- Chou, P. Y. & Fasman, G. D. (1978). Prediction of the secondary structure of proteins from their amino acid sequence. *Advan. Enzymol. Relat. Subj. Biochem.* **47**, 45–148.
- Clarke, N. D., Kissinger, C. R., Desjarlais, J., Gilliland, G. L. & Pabo, C. O. (1994). Structural studies of the engrailed homeodomain. *Protein Sci.* **3**, 1779–1787.
- Cohn, E. J. & Edsall, J. T. (1943). *Proteins, Amino Acids and Peptides as Ions and Dipolar Ions*, pp. 370–381, Reinhold Publishing Corporation, New York.
- Dahiyat, B. I. & Mayo, S. L. (1997). *De novo* protein design: fully automated sequence selection. *Science*, **278**, 82–87.
- Duckworth, H. W., Jaenicke, R., Perham, R. N., Wilkie, A. O. M., Finch, J. T. & Roberts, G. C. K. (1982). Limited proteolysis and proton NMR spectroscopy of *Bacillus stearothermophilus* pyruvate dehydrogenase multienzyme complex. *Eur. J. Biochem.* **124**, 63–89.
- Gonzalez, L., Jr, Woolfson, D. N. & Alber, T. (1996). Buried polar residues and structural specificity in the GCN4 leucine zipper. *Nature Struct. Biol.* **3**, 1011–1018.
- Hendsch, Z. S. & Tidor, B. (1994). Do salt bridges stabilize proteins? A continuum electrostatic model. *Protein Sci.* **3**, 211–226.
- Johnson, M. L., Correia, J. J., Yphantis, D. A. & Halverson, H. R. (1981). Analysis of data from the

- analytical ultracentrifuge by nonlinear least-squares techniques. *Biophys. J.* **36**, 575–588.
- Kalia, Y. N., Brocklehurst, S. M., Hipps, D. S., Appella, E., Sakaguchi, K. & Perham, R. N. (1993). The high-resolution structure of the peripheral subunit-binding domain of dihydrolipoamide acetyltransferase from the pyruvate dehydrogenase multienzyme complex of *Bacillus stearothermophilus*. *J. Mol. Biol.* **230**, 323–341.
- Kay, M. S. & Baldwin, R. L. (1996). Packing interactions in the apomyoglobin folding intermediate. *Nature Struct. Biol.* **3**, 439–445.
- Kelley, L. A., Gardner, S. P. & Sutcliffe, M. J. (1996). An automated approach for clustering an ensemble of NMR-derived protein structures into conformationally related subfamilies. *Protein Eng.* **9**, 1063–1065.
- Kraulis, P. J. (1991). MOLSCRIPT: a program to produce both detailed and schematic plots of protein structures. *J. Appl. Crystallog.* **24**, 946–950.
- Kraulis, P. J., Jonasson, P., Nygren, P.-Å., Uhlen, M., Jendeberg, L., Nilsson, B. & Kordel, J. (1996). The serum albumin-binding domain of streptococcal protein G is a three-helical bundle: a heteronuclear NMR study. *FEBS Letters*, **378**, 190–194.
- Kuwajima, K. (1989). The molten globule state as a clue for understanding the folding and cooperativity of globular protein structure. *Proteins: Struct. Funct. Genet.* **6**, 87–103.
- Lumb, K. J. & Kim, P. S. (1995). A buried polar interaction imparts structural uniqueness in a designed heterodimeric coiled coil. *Biochemistry*, **34**, 8642–8648.
- Lyu, P. C., Gans, P. L. & Kallenbach, N. R. (1992). Energetic contribution of solvent-exposed ion pairs to alpha-helix structure. *J. Mol. Biol.* **223**, 343–250.
- Manning, M. C. & Woody, R. W. (1991). Theoretical CD studies of polypeptide helices: examination of important electronic and geometric factors. *Biopolymers*, **31**, 569–586.
- McKnight, C. J., Doering, D. S., Matsudaira, P. T. & Kim, P. S. (1996). A thermostable 35-residue subdomain within villin headpiece. *J. Mol. Biol.* **260**, 126–134.
- McKnight, C. J., Matsudaira, P. T. & Kim, P. S. (1997). NMR structure of the 35-residue villin headpiece subdomain. *Nature Struct. Biol.* **4**, 180–184.
- Morozova, L. A., Jaumoe, D. T., Arico-Muendel, C., Van Dael, H. & Dobson, C. M. (1995). Structural basis of the stability of a lysozyme molten globule. *Nature Struct. Biol.* **2**, 871–875.
- Munoz, V. & Serrano, L. (1994). Elucidating the folding problem of helical peptides using empirical parameters. *Nature Struct. Biol.* **1**, 399–409.
- Munoz, V. & Serrano, L. (1995a). Elucidating the folding problem of helical peptides using empirical parameters. II. Helix macrodipole effects and rational modification of the helical content of natural peptides. *J. Mol. Biol.* **245**, 275–296.
- Munoz, V. & Serrano, L. (1995b). Elucidating the folding problem of helical peptides using empirical parameters. III. Temperature and pH dependence. *J. Mol. Biol.* **245**, 297–308.
- Myers, J. K., Pace, C. N. & Scholtz, J. M. (1995). Denaturant *m* values and heat capacity changes: relation to changes in accessible surface areas of protein unfolding. *Protein Sci.* **4**, 2138–2148.
- Nobbs, T. J., Cortés, A., Gelpi, J. L., Holbrook, J. J., Atkinson, T., Scawen, M. D. & Nicholls, D. J. (1994). Contribution of a buried aspartate residue towards the catalytic efficiency and structural stability of *Bacillus stearothermophilus* lactate dehydrogenase. *Biochem. J.* **300**, 491–499.
- O'Neil, K. T. & DeGrado, W. F. (1990). A thermodynamic scale for the helix-forming tendencies of the commonly occurring amino acids. *Science*, **250**, 646–651.
- Pace, C. N., Shirley, B. A. & Thomson, J. A. (1990). Measuring the conformational stability of a protein. In *Protein Structure: A Practical Approach* (Creighton, T. E., ed.), pp. 311–330, Oxford University Press, Oxford.
- Packman, L. C., Borges, A. & Perham, R. N. (1988). Amino acid sequence analysis of the lipoyl and peripheral subunit-binding domains in the lipoyl acetyltransferase component of the pyruvate dehydrogenase complex from *Bacillus stearothermophilus*. *Biochem. J.* **252**, 79–86.
- Privalov, P. L. (1992). Physical basis of the stability of the folded conformations of proteins. In *Protein Folding* (Creighton, T. E., ed.), pp. 83–126, W. H. Freeman and Company, New York.
- Privalov, P. L. & Gill, S. J. (1988). Stability of protein structure and hydrophobic interaction. *Advan. Protein Chem.* **39**, 191–234.
- Ptitsyn, O. (1996). How molten is the molten globule? *Nature Struct. Biol.* **3**, 488–490.
- Raiford, D. S., Fisk, C. L. & Becker, E. D. (1979). Calibration of methanol and ethylene glycol nuclear magnetic resonance thermometers. *Anal. Chem.* **51**, 2050–2051.
- Raleigh, D. P., Betz, S. F. & DeGrado, W. F. (1995). A *de novo* designed protein mimics the native state of natural proteins. *J. Am. Chem. Soc.* **117**, 7558–7559.
- Rohl, C. A. & Baldwin, R. L. (1997). Comparison of NH exchange and circular dichroism as techniques for measuring the parameters of the helix-coil transition in peptides. *Biochemistry*, **36**, 8435–8442.
- Scholtz, J. M., Quian, H., Robbins, V. H. & Baldwin, R. L. (1993). The energetics of ion-pair and hydrogen bonding interactions in a helical peptide. *Biochemistry*, **32**, 9668–9676.
- Schueler, O. & Margalit, H. (1995). Conservation of salt bridges in protein families. *J. Mol. Biol.* **248**, 125–135.
- Spolar, R. S., Livingstone, J. R. & Record, M. T., Jr (1992). Use of liquid hydrocarbon and amide transfer data to estimate contributions to thermodynamic functions of protein folding from the removal of nonpolar and polar surface from water. *Biochemistry*, **31**, 3947–3955.
- Starovasnik, M. A., Braisted, A. C. & Wells, J. A. (1997). Structural mimicry of a native protein by a minimized binding domain. *Proc. Natl Acad. Sci. USA*, **94**, 10080–10085.
- Struthers, M. D., Cheng, R. P. & Imperiali, B. (1996). Economy in protein design: evolution of a metal-independent $\beta\beta\alpha$ motif based on the zinc finger domains. *J. Am. Chem. Soc.* **118**, 3073–3081.
- Tan, Y.-J., Oliveberg, M., Davis, B. & Fersht, A. R. (1995). Perturbed pK_a values in the denatured states of proteins. *J. Mol. Biol.* **254**, 980–992.
- Tanford, C. (1970). Protein denaturation. Part C. Theoretical models for the mechanism of denaturation. *Advan. Protein Chem.* **24**, 1–95.

- Vriend, G. (1990). WHAT IF: a molecular modeling and drug design program. *J. Mol. Graph.* **8**, 52–56.
- Wilkstrom, M., Drakenberg, T., Forsen, S., Sjobring, U. & Bjorck, L. (1994). Three-dimensional solution structure of an immunoglobulin light chain-binding domain of protein L. Comparison with the IgG-binding domain of protein G. *Biochemistry*, **33**, 1401–14017.
- Wojcik, J., Altmann, K.-H. & Scheraga, H. A. (1990). Helix-coil stability constants for the naturally occurring amino acids in water. XXIV. Half-cystine parameters from random poly(hydroxybutylglutamine-co-S-methylthio-L-cysteine). *Biopolymers*, **30**, 121–134.
- Woody, R. W. (1978). Aromatic side-chain contributions to the far ultraviolet circular dichroism of peptides and proteins. *Biopolymers*, **17**, 1451–1567.
- Yu, H., Rosen, M. K., Shin, T. B., Seidel-Dugan, C., Brugge, J. S. & Schreiber, S. L. (1992). Solution structure of the SH3 domain of src and identification of its ligand-binding site. *Science*, **258**, 1665–1668.

Edited by P. E. Wright

(Received 22 July 1997; received in revised form 28 October 1997; accepted 6 November 1997)